



HAL
open science

Agglomeration of wheat powders by a novel reverse wet agglomeration process

E. Rondet, Bernard Cuq, Denis Cassan, Thierry Ruiz

► To cite this version:

E. Rondet, Bernard Cuq, Denis Cassan, Thierry Ruiz. Agglomeration of wheat powders by a novel reverse wet agglomeration process. *Journal of Food Engineering*, 2016, 173, pp.92-105. 10.1016/j.jfoodeng.2015.10.046 . hal-01261000

HAL Id: hal-01261000

<https://hal.science/hal-01261000>

Submitted on 27 May 2020

HAL is a multi-disciplinary open access archive for the deposit and dissemination of scientific research documents, whether they are published or not. The documents may come from teaching and research institutions in France or abroad, or from public or private research centers.

L'archive ouverte pluridisciplinaire **HAL**, est destinée au dépôt et à la diffusion de documents scientifiques de niveau recherche, publiés ou non, émanant des établissements d'enseignement et de recherche français ou étrangers, des laboratoires publics ou privés.

Accepted Manuscript

Agglomeration of wheat powders by a novel reverse wet agglomeration process

E. Rondet, B. Cuq, D. Cassan, T. Ruiz

PII: S0260-8774(15)30047-9

DOI: [10.1016/j.jfoodeng.2015.10.046](https://doi.org/10.1016/j.jfoodeng.2015.10.046)

Reference: JFOE 8389

To appear in: *Journal of Food Engineering*

Received Date: 14 July 2015

Revised Date: 14 September 2015

Accepted Date: 29 October 2015



Please cite this article as: Rondet, E., Cuq, B., Cassan, D., Ruiz, T., Agglomeration of wheat powders by a novel reverse wet agglomeration process, *Journal of Food Engineering* (2015), doi: 10.1016/j.jfoodeng.2015.10.046.

This is a PDF file of an unedited manuscript that has been accepted for publication. As a service to our customers we are providing this early version of the manuscript. The manuscript will undergo copyediting, typesetting, and review of the resulting proof before it is published in its final form. Please note that during the production process errors may be discovered which could affect the content, and all legal disclaimers that apply to the journal pertain.

Comment citer ce document :

Rondet, E., Cuq, B., Cassan, D., Ruiz, T. (2016). Agglomeration of wheat powders by a novel reverse wet agglomeration process. *Journal of Food Engineering*, 173, 92-105. DOI : [10.1016/j.jfoodeng.2015.10.046](https://doi.org/10.1016/j.jfoodeng.2015.10.046)

Agglomeration of wheat powders by a novel reverse wet agglomeration process

Rondet E. ⁽¹⁾, Cuq B. ⁽²⁾, Cassan D. ⁽²⁾ and Ruiz T. ⁽²⁾

¹ UMR 95 QUALISUD, Université de Montpellier,
Faculté de Pharmacie, Laboratoire de Physique Moléculaire et Structurale, 15 avenue Charles
Flahault, 34093 Montpellier cedex 5, France

² UMR 1208 IATE, Montpellier SupAgro, Université de Montpellier, INRA, CIRAD
2 place Viala, 34000 Montpellier, France
eric.rondet@univ-montp1.fr

Abstract - The wet agglomeration process is implemented to improve the powders functionalities. The objective of the present work is to investigate a novel reverse wet agglomeration process for reactive powders. This novel process is conducted in two main successive phases during mechanical mixing. The first phase consists of mixing a specific amount of powder and water to produce a continuous saturated paste, called dough, by controlling the physicochemical reactivity of the biochemical components of the powder. The second stage consists of generating the agglomerates by adding the powder inside the continuous dough under mixing conditions. This agglomeration process is mainly promoted by fragmentation mechanism. We have evaluated the impact of the process conditions on the electric consumption, agglomeration yield and characteristics of the agglomerates. Experiments were conducted using durum wheat semolina as raw materials. The results were compared to those obtained by using the classical wet agglomeration process, at same final water content of the agglomerates.

Keywords - Reverse agglomeration, fragmentation mechanisms, electric consumption, wheat powders, compactness, microstructure.

33 **1. INTRODUCTION**

34 Agglomeration is a unit operation, which is implemented to improve the powders
35 functionalities relating to flow properties, dust generation, mixing capacity, solubility, *etc.*, by
36 increasing the size of structures. During agglomeration, native particles are gathered to form
37 larger assemblies, called the agglomerates. Wet controlled growth agglomeration refers to
38 agglomeration processes during which a liquid binder is sprayed over an agitated powder bed
39 (Ennis et al., 1991; Iveson et al., 2001). Knowledge about the agglomeration process of food
40 powders still remains partial, although significant scientific works have been conducted over
41 the last 15 years (Litster and Ennis, 2004; Saleh and Guigon, 2009; Palzer, 2011; Cuq et al.,
42 2013). The description of the mechanisms, which are involved during the agglomeration of
43 the food powders, still represents a real scientific stake.

44
45 The wet agglomeration of powders requires the addition of water to generate capillary bridges
46 which adds cohesion between particles. Agglomeration mechanisms result from the spatial
47 arrangement of the native particles with the binder components, promoting attractive
48 interactions and links. The contribution of liquid bridges between native particles largely
49 overtakes the physical forces and the van der Waals interactions (Hapgood et al., 2003). For
50 food powders, besides the contribution of physical phenomena, the mechanisms also depend
51 on the physicochemical reactivity of the molecules, which strengthens the adhesion forces
52 between particles, by adding a significant contribution of the viscous forces (Cuq et al., 2013).
53 When the food powders are subjected to the addition of water, and/or to mechanical stresses,
54 the molecules are able to undergo the glass transition and/or irreversible physicochemical
55 changes (*e.g.* solubilisation, denaturation, diffusion, *etc.*). The process conditions, including
56 mechanical stress, temperature, water addition, and process time, greatly determine the
57 effective contribution of the physicochemical reactivity of the molecules (Cuq et al., 2013).
58 Based on their chemical composition, food molecules have the capacity to establish, between
59 themselves and with the surrounding molecules, interactions of different energies. Low
60 energy interactions include hydrogen bonds, hydrophobic interactions, and ionic interactions,
61 while covalent bonds such as disulfide bonds represent high energy interactions. These
62 interactions contribute to defining their capacity to react when subjected to water addition
63 and/or heat treatments. For examples, the wheat proteins can establish continuous
64 macromolecular network when subjected to water addition and mixing, and they can establish
65 irreversible intermolecular covalent bonds, under heat treatments, that contribute to
66 irreversible reticulation mechanisms (Abecassis et al., 2012).

67

68 Wet agglomeration is generally described as a combination of three processes at different
69 rates: wetting-nucleation, consolidation-growth, and attrition-breakage (Iveson et al., 2001).

70 The apparent rate of the agglomeration depends on the specific contribution of each
71 processes. The growth mechanisms depend on the opposite contributions of cohesion and
72 rupture mechanisms. The cohesion forces generate interactions between particles, while the
73 rupture forces and the local shearing effects lead to breakage. The mechanisms of attrition and
74 breakage help to improve homogeneity and strength of the granules by promoting
75 consolidation, in addition to the obvious growth retardation (Reynolds et al., 2005).

76 Recent works have investigated the interest to consider the mechanisms of breakage and
77 fragmentation as a major way to produce agglomerates. Rondet (2008) was the first to
78 develop a reverse agglomeration process applied on three different powders (microcrystalline
79 cellulose, calcium phosphate, and kaolin) classically used for pharmaceutical applications.
80 The first stage of the process is the preparation of a wet saturated paste by mixing the native
81 powder with high amounts of water. The second phase consists of adding the native powder
82 inside the paste during mixing, in order to promote the fragmentation mechanisms and
83 generate the agglomerates with controlled water content. The authors demonstrated the
84 reversibility of the paste transition, between the discrete granular state and the continuous
85 paste state. The paste transition was identified at a specific range of water contents, close to
86 the plastic limits of the powders. The agglomerates are more spherical and compact than those
87 produced by the classical wet agglomeration process.

88 In 2010, a reverse wet granulation process was patented for pharmaceutical uses (Li et al.,
89 2010). Granules are formed by incorporating a mixture of dry powders (*i.e.* the excipients)
90 into the drug-polymer slurry (*i.e.* the active pharmaceutical ingredient), and by drying the
91 products. The granules formed comprise a core containing the active pharmaceutical
92 ingredient having poor aqueous solubility.

93 Recently, Wade et al. (2013, 2014, 2015) developed a novel reverse-phase wet granulation
94 process for pharmaceutical applications, based on the immersion of the dry powder mix, into
95 the binder liquid. From a slurry state, the addition of the powder mass enables mechanical
96 distribution of binder liquid to take place, until the desired particle size is obtained, through
97 controlled breakage. The main mechanisms are supposed to be breakage of the large saturated
98 agglomerates. The binder liquid is dispersed throughout the powder by mechanical
99 distribution. This novel approach is supposed to have the potential advantages of eliminating
100 the traditional variations associated to the stage of granule nucleation, and of reducing the

101 potential risk of uncontrolled growth of the granules. They evaluated the effects of: liquid
102 saturation, binder liquid viscosity, and impeller speed on the physical and end-uses properties
103 of the granules.

104
105 The objective of the present paper is to investigate the novel reverse wet agglomeration
106 process by fragmentation of a pasty state, in the specific case of reactive powders, able to
107 form a continuous dough stabilized by a molecular protein network. Durum wheat semolina
108 was used as reactive powder for the present study. The novel process is conducted as two
109 main successive phases, during continuous mechanical mixing. The first stage consists of
110 mixing a specific amount of powder and water to produce a continuous saturated paste, called
111 the dough, by controlling the physicochemical reactivity of the biochemical components of
112 the powder. This paste could not be considered as a granular suspension because the original
113 granular state of the native particles is lost. While the cohesion of the granular paste is almost
114 reversible in the previous works (Rondet, 2008), the presence of reactive proteins of the wheat
115 (i.e. gluten) in the particles of durum wheat semolina led the formation of a dough stabilized
116 by a biochemical molecular network and the irreversible loss of the native granular state. The
117 second stage consists of ~~in~~ generating the agglomerates, by adding the dry powder inside the
118 continuous dough, during the mixing. The fragmentation mechanisms induce dough
119 disruption and agglomerates production.

120 We have evaluated the impact of the process conditions on the electric consumption,
121 agglomeration yield and characteristics of the agglomerates. Experiments have been
122 conducted by using durum wheat semolina as raw materials. Durum wheat semolina is a
123 reactive powder able to form a continuous protein network, when it is wetted and
124 mechanically sheared (Pollini et al., 2012). The physicochemical reactivity was controlled by
125 the water content of the dough. Two conditions have been tested: low reactivity at low water
126 content of the dough (above the plastic state) and high reactivity at high water content of the
127 dough (above the pseudo-liquid state). The results are compared to those obtained by using
128 the classical wet agglomeration process, at the same final water contents of the agglomerates.

129
130

131 **2. MATERIAL AND METHODS**

132

133 **2.1. Raw materials**

134 Durum wheat semolina of industrial quality (Panzani group, France) was used as raw material
135 for the agglomeration experiments. Semolina was stored in hermetic containers at 4°C until
136 experiments were carried out.

137 Semolina was first characterized using standardized methods. The water content of semolina
138 (16.4 ± 0.5 g water/100 g dry semolina) was determined according to the approved method 44-
139 15A (AACC, 2000), by weighing after oven drying (RB 360, WC Heraeus GmbH, Hanau,
140 Germany) at 105°C for 24 h. The total nitrogen content (TN) of semolina was determined by
141 the Kjeldahl method, and the crude protein content (12.4 g protein/100 g dry matter) was
142 calculated according to $TN \times 5.7$ based on the AFNOR method V 03-050 (AFNOR, 1970).
143 Median value of particle diameter of semolina ($d_{50} = 287 \pm 8 \mu\text{m}$) was measured by using laser
144 granulometry (Coulter TMLS 230, Malvern, England) at room temperature. The diameter
145 span ($(d_{90}-d_{10})/d_{50}$) was 1.56. The semolina true density ($1.478 \pm 0.005 \text{ g}\cdot\text{cm}^{-3}$) was measured
146 by helium pycnometry.

147 Liquid limit and plastic limit, which correspond to Atterberg tests used in soil science (Holtz
148 and Kovacs, 1981) are carried out on semolina in accordance with the French P 94-051 and P
149 94-052-1 methods (AFNOR, 1993, 1995). For granular media, the plastic limit (w_p) is the
150 water content which gives the transition between the solid and the plastic state. The liquid
151 limit (w_L) is the water content which gives the transition between the plastic and the pseudo-
152 liquid state. The plastic and liquid limit values are measured at respectively 59% and 76% for
153 the durum wheat semolina. The plasticity index (w_L-w_p) is equal to 17% and allows
154 assimilating the durum wheat semolina at a plastic organic soil like plastic silt (Holtz and
155 Kovacs, 1981).

156

157 2.2. Agglomeration processes

158 The present work specifically investigates the effect of two different agglomeration paths (the
159 direct classical wet agglomeration process and the reverse agglomeration process), by using a
160 low shear planetary mixer (Fig. 1).

161 *The direct classic wet agglomeration process* is conducted by spraying water directly
162 on the native powder inside the mixer bowl, during the mechanical mixing (Fig. 1). Water
163 spraying is conducted until reaching the defined water content (i.e. the process water content),
164 of the wet agglomerates (30, 40, or 50%).

165 *The reverse agglomeration process* is conducted with two successive steps. A part of
166 the native semolina powder is first mixed in the mixer bowl. The first step consists of
167 generating the continuous wet dough in the mixer bowl, by adding the defined amounts of

168 water on the native semolina, during the mechanical mixing. Water addition is conducted
169 until reaching the defined water contents, to produce the plastic dough (at 75% water content)
170 or the pseudo-liquid dough (at 110% water content) (Fig. 1). The second step corresponds to
171 the formation of the powders by fragmentation mechanisms, lead by the addition of the native
172 powder. The native powder was poured on the free surface of the dough and incorporated
173 inside by the mechanical mixing. The amount of the added powder is defined to reach the
174 final water content of the wet agglomerates (30, 40, or 50%).

175 We tested 9 different experimental conditions, which are associated to the 3 process paths and
176 to the 3 final water contents of the agglomerates. The reproducibility of the process paths was
177 checked by realizing some experiments in triplicate, at least one for each different process
178 path. Experiments were done by using a batch planetary mixer (Kenwood Major 1200),
179 equipped with a fixed bowl of 5 liters and a K blade that rotates around a vertical axis. All the
180 experiments were conducted with the constant final load (1.5 kg) of the wet agglomerates and
181 the constant rotation speed of the blade (70 rpm), to promote the conditions of low shear and
182 constant total time of mixing (12 min). The electric consumption of the mixer was
183 continuously measured by using a wattmeter (Wattcom[®]). Before the start of the experiments,
184 we have conducted a stage of no-load mixing, at 70 rpm during a long enough duration (i.e.
185 30 min) to reach steady state conditions of the electric consumption of the mixer (Fig. 2). The
186 initial load of the native powder (Table 1) was rapidly poured inside the mixer bowl and
187 mixed for 2 min. During the wetting stage (Fig. 2), performed during the mixing, water was
188 directly sprayed on the free surface of the powder bed at constant flow rate (5.25 mL.s⁻¹) by
189 using a flat spray nozzle (TPU650017, Spraying System Emani, France) connected to the
190 water supply network. The diameter of the water droplets were estimated to 50-100 µm
191 (Mandato et al., 2012). In these conditions, the dimensionless spray flux was estimated to be
192 around 0.2. This value is slightly higher than the threshold value (0.1) that distinguishes the
193 nucleation regime by the drop controlled, in the nucleation regime map as defined by
194 Hapgood et al. (2003).

195 For the direct process, the spraying time (~~30-63 see~~) was defined to incorporate the
196 necessary mass of water (Table 1) to reach the water content of the final agglomerates. After
197 the spraying phase, the wet agglomerates were mixed until a total time of process of 12 min
198 (Fig. 2).

199 For the reverse processes, the first stage of the formation of the continuous dough is
200 conducted during a constant time of 2 min. During this stage, the spraying time was defined to
201 incorporate the necessary mass of water (Table 1) to reach the defined water content of the

202 continuous dough (Fig. 2). During the following fragmentation stage, the addition of the
203 powder was conducted at constant feeding rate ($8.7 \text{ g}\cdot\text{sec}^{-1}$) by using a weight feeder (K-SFS-
204 24, K-TRON, New Jersey, USA), which was directly placed above the mixer bowl. The time
205 for the addition of the powder was defined to incorporate the necessary mass of powder
206 (Table 1) to reach the water content of the wet agglomerates. After the powder addition phase,
207 the wet agglomerates were mixed until a total process time of 12 min.

208
209 The wet agglomerates were characterized according to their size distribution immediately
210 after the processing. 100 g of product was sampled inside the mixer and poured over a column
211 of 11 sieves of decreasing mesh size (10, 5.6, 2, 1.25, 0.9, 0.8, 0.71, 0.63, 0.5, 0.4, and 0.315
212 mm). The sieve column was moved by gentle manual stirring for 1 min to separate the
213 agglomerate fractions. The repartition of the fractions on each sieve was measured by
214 weighing. The size distribution was expressed as the percent of total weight. Even if the
215 particle size distribution curves were not unimodal, the apparent median diameter (d_{50}) and
216 apparent span ($((d_{90}-d_{10}) / d_{50})$) of the size distribution were calculated as global apparent
217 descriptors, that could under or over-represent the trend.

218 219 2.2. Consolidation and stabilization of the agglomerates

220 After the agglomeration stage, the wet agglomerates were consolidated by the steaming stage
221 and they were stabilized by the drying stage. The stages of steaming and drying were only
222 conducted on the wet agglomerates that were sampled between the sieves of 1.25 and 2 mm
223 mesh size. We made this choice, because it corresponds to one of the fields of application
224 expected for our works: the manufacturing of the agglomerated couscous grains of durum
225 wheat (Abecassis et al., 2012). Obviously, the knowledge of the properties of this fraction
226 does not allow describing the properties of the larger or smaller fractions.

227 Immediately after sieving, the agglomerates were spread as a thin layer (about 3 mm) over a
228 stainless steel plate, inside a steam cooker of 20 L (Ravant Chaudronnerie, France). The stage
229 of steaming was conducted for 15 min at 100°C , under saturated steam flow of $20 \text{ kg}\cdot\text{h}^{-1}$, and
230 at atmospheric pressure. The steamed agglomerates were immediately dried as a thin layer
231 (about 3 mm) over stainless steel mesh, by using a pilot scale dryer (Afrem, Lyon, France).
232 The drying was conducted for 60 min at 70°C and at 80% relative humidity. The dried
233 agglomerates were collected and stored inside hermetic plastic cups until characterization.

234 235 2.3. Characterization of the (wet and dried) agglomerates

236

237 Water content - The water content was determined on 3-5 g samples, by a drying method in
 238 an oven (RB 360, WC Heraeus GmbH, Hanau, Germany) at 105°C for 24 h (AACC Method
 239 44-15A). Mean values were determined from triplicate.

240

241 Compactness - The solid mass (m_{Solid} ; g dry matter) was first calculated from the weight
 242 values of the agglomerates (m ; g) and their water content (w ; g water / g dry matter)..

$$243 \quad m_{Solid} = \frac{m}{1+w} \quad (1)$$

244 The density of the agglomerates (ρ ; g.cm⁻³) was determined by using a hydrostatic balance
 245 (Precisa serie 321 LX 120A SCS, equipped with kit for determining density for solid and
 246 liquid) and using paraffin oil. The solid volume fraction of the agglomerates (ϕ ; cm³ solid
 247 matter / cm³) was calculated using Eq. (2).

$$248 \quad \phi = \frac{V_{Solid}}{V} = \frac{\rho}{\rho_{Solid}^*(1+w)} \quad (2)$$

249 Where V_{Solid} is the volume of the solid matter of the agglomerates (cm³ solid matter) and
 250 ρ_{Solid}^* is the true density of material (1.478 ±0.005 g.cm⁻³) measured by helium pycnometry.
 251 Mean values were determined from triplicate.

252

253 Shearing properties - Shearing properties of the wet agglomerates were measured using the
 254 FT₄ powder rheometer (Freeman Technology, Worcestershire, UK) according to Rondet et al.
 255 (2013). Measurements were carried out in a cylindrical glass cell (diameter = 50 mm; height =
 256 50 mm) and the FT₄ probe (with a helix of a -5° angle and a diameter of 23.5 mm). The
 257 sample was subjected to a pre-shearing stage (0.3°.s⁻¹ on 60° with a pressure of 15 kPa)
 258 carried out with the FT₄ powder rheometer shearing probe. Four shearing cycles were carried
 259 out for various normal stresses (1.75, 1.5, 1.25, and 1 kPa), at a speed of 0.3°.s⁻¹. Failure shear
 260 stress was recorded for each studied normal stress. Undrained shearing tests were analysed
 261 using Mohr's representation of the plane stress state with the normal stress (σ , kPa) and the
 262 shearing stress (τ , kPa). The shearing properties were described using the Mohr-Coulomb
 263 rupture criterion.

$$264 \quad \tau = \mu\sigma + c \quad (3)$$

265 where μ is the friction coefficient (dimensionless) and c is the cohesion (kPa). The friction
 266 coefficient is the slope and cohesion is the intercept with the y-axis of the linear relationship
 267 between σ and τ . Experiments were carried out in triplicate.

268

269 Scanning electron microscopy - The microstructure of the dried agglomerates was observed
 270 by scanning electron microscopy (JSM-T2000, JEOL, Tokyo, Japan). A sample was mounted
 271 in epoxy resin and coated by gold to provide the conductivity and the emission of secondary
 272 electron. For each sample, pictures with different magnifications were taken.

273
 274 Color – A sample of dried agglomerates was densely packed in a cylindrical glass cell (6 cm
 275 diameter and 2 cm thickness) and levelled off. Color coordinates (L* lightness, a* redness,
 276 and b* yellowness) were measured directly by using a reflectance colorimeter (Konica
 277 Minolta CR - 410, France) with the calibration to daily light (D65). Colours measurements
 278 were carried out in triplicate on three different samples. The arithmetic means of the
 279 coordinates were calculated together with total color difference.

$$280 \quad \Delta E = \sqrt{\sum(x_i - x_0)^2} \quad (4)$$

281 Where x is L*, a* or b*, and i refers to the different products and 0 means durum wheat
 282 semolina as standard.

283
 284 Swelling capacity – The swelling capacity of the dried agglomerates was measured according
 285 to Guezlane and Abecassis (1991). A sample (20 g \pm 0.1 g) was placed inside a graduated 100
 286 mL test tube (25 cm long and 3 cm diameter) containing 50 mL of distilled water. The test
 287 tube was sealed and turned upside down 10 times successively. Water at 20°C was carefully
 288 added to wash down the agglomerates stuck to the internal sidewall of the test tube, until the
 289 final volume of the mixture reached 100 mL. The test tube was then placed at room
 290 temperature for 30 min. The volume of solid hydrated "phase" was directly read on the tube.
 291 Measurements were realized in triplicate. The swelling capacity criterion at 20°C (ml.g⁻¹)
 292 corresponded to the ratio the final volume of the hydrated agglomerates (V; ml) over the
 293 initial mass of agglomerates (M; g).

$$294 \quad S_{20^\circ\text{C}} = 100 \frac{V}{M} \quad (5)$$

296 2.4. Statistical analysis

297
 298 The statistical significance of results was assessed using single-factor analysis of variance
 299 (ANOVA). Multiple comparisons were performed by calculating the least significant
 300 difference using Microsoft Excel 2011, at a 5% significance level.

301

302

303 **3. RESULTS**

304 The comparison of the direct or reverse agglomeration processes was conducted by both
305 monitoring the energy consumption during the processing and by measuring the
306 characteristics of the wet agglomerates and of the dried agglomerates.

307

308 **3.1. Electric consumption during process**

309 The electric consumption of the mixer was measured during the successive stages of the
310 agglomeration processes. During the first stage of no-load mixing, we observed a small peak
311 of electric input power, followed by a progressive decrease of the electric power until it reach
312 a constant value, in steady state conditions (data not presented). According to Rondet et al.
313 (2012), the electric input power during the no-load mixing is the sum of the mechanical
314 output power for rotating the blade and of the dissipation terms (heat dissipation, motor
315 magnetic dissipation, and motor mechanical dissipation). The measured values of the electric
316 input power were normalized by subtracting the plateau value measured at the end of the stage
317 of no-load mixing (Rondet et al., 2012).

318 During the mixing of the initial load of the native powder (Fig. 3), the normalized electric
319 input power values are low. These values (Table 2) are correlated ($R^2 = 0.988$) with the
320 weight of the native powder in the mixer tank before the water addition (Table 1), except
321 when the initial load is too low (less than 400 g load), compared to the mixer size.

322

323 During the agglomeration stage, the curves of the normalized electric input power are specific
324 of the process. For the direct agglomeration process (Fig. 3A), the electric input power rapidly
325 increases during the spraying of the water (stage 3), due to the increase in cohesion between
326 the particles (Rondet et al., 2013). The electric input power reaches a maximum value at the
327 end of the stage of water spraying, and then progressively decreases during the final stage of
328 mixing, and reaches a final plateau value.

329 For the reverse agglomeration processes (Fig. 3B-C), we first observe an increase in the
330 electric input power during the stage of water spraying (stage 3), due to the formation of the
331 continuous dough. For the plastic dough conditions (Fig. 3B), the power curve is
332 characterized by a high peak and large bandwidth due to the high consistency of the dough.
333 For the pseudo-liquid dough conditions (Fig. 3C), the power curve is characterized by a slight
334 increase and small bandwidth, due to the liquid behaviour and low consistency of the dough.

335 When starting the final stage of powder addition, we first can observe a short transitory phase

336 with fluctuations of the electric input power, due to the lubricant effect of the added particles,
337 which are not incorporated inside the dough structure. The addition of powder induces a rapid
338 increase of the electric input power (Fig. 3B-C), due to the increase of the dry matter content
339 of the dough: the continuous dough becomes more cohesive. Similar increases in the cohesion
340 of wheat semolina dough with decreasing water contents were observed by Rondet et al.
341 (2013). They identified a maximum dough cohesion value near 52% water content (i.e. the
342 plastic limit), which is the limit water content, at the structure transition from the continuous
343 dough to the granular pasta. Below 52%, the decrease of the water content decreases the
344 values of the cohesion of the discrete granular cohesive medium. During the reverse
345 agglomeration process (Fig. 3BC), we also observe that final powder addition decreases the
346 electric power values, due to the transition from the continuous dough to the discrete granular
347 cohesive medium. During the final period of mixing (Fig. 3BC), the electric input power
348 continues to slightly decrease and reaches a final plateau value.

349 Whatever the processes, increases in the water content (from 30 to 50%) of the wet powders
350 increase the values of the electric power measured at the end of the process (Table 2). This is
351 due to the increase in the cohesion between the wet agglomerates (Rondet et al., 2013).

352
353 The measured values of the normalized electric input power were used to calculate the electric
354 energy consumption during each stage of the process (Table 2). For the direct agglomeration
355 process, the values of the total energy consumption are low (11-27 kJ), because the products
356 still stay in a powdered granular state with low cohesion forces, which were determined at 4
357 to 11 kPa for the water contents ranging from 30% to 50% (Rondet et al., 2013). These forces
358 are low when comparing to the wheat dough with continuous protein network, whatever the
359 end water content of the wet agglomerates.

360 For the reverse agglomeration processes, the mixing of the continuous dough during the
361 stages of water addition and of fragmentation requires higher level of mechanical energy
362 (Table 2). Whatever the water content, the total energy consumption for the liquid dough
363 conditions (13-38 kJ) is slightly higher than those measured for the direct process. The level
364 of viscosity of the continuous pseudo-liquid dough does not require high levels of electric
365 energy. On the other hand, the total energy consumption for plastic dough conditions (21-61
366 kJ) are largely higher than those measured for the direct process. The cohesive behaviour of
367 the plastic dough requires high level of electric energy during the stage of mixing, whatever
368 the end water content of the wet agglomerates.

369

370 **3.2. Characteristics of the wet agglomerates**

371 To compare the agglomeration processes, we have measured the distribution of the size
372 properties and of the hydro-textural characteristics of the wet agglomerates (diameter, water
373 content, and compactness).

374

375 3.2.1. Size distribution

376 The agglomeration processes generate agglomerates with dispersed sizes. Whatever the
377 processes and the water contents, the end size distribution display multimodal shapes curves
378 (Fig. 4-5). The size distributions of the wet agglomerates were here described by considering
379 four classes of agglomerates according to their diameter: small ($d < 0.4$ mm), medium ($0.4 <$
380 $d < 0.71$ mm), large ($0.71 < d < 1.25$ mm), and very large (1.25 mm $< d$) agglomerates (Fig.
381 6). Even if the distribution curves of diameter did not display unimodal normal shape, we
382 calculated the apparent median diameter (d_{50}) and apparent dispersion parameter (span) as
383 global criteria (Fig. 7).

384 The results demonstrated a significant impact of the process on the slope of the size
385 distribution curves (Fig. 4), whatever the water content. The reverse plastic process is
386 characterized by the agglomerates with slightly lower values of the apparent median
387 diameters (-90 μ m) and of the apparent span, compared to the direct process (Fig. 7). On the
388 other hand, the reverse liquid process is characterized by agglomerates with slightly higher
389 values of the apparent median diameters ($+115$ μ m), and lower values of the apparent span,
390 compared to the direct process. These effects can be mainly observed at 30% and 50%
391 content, albeit with a greater difference at 50% level. We cannot give explanation into why at
392 40% the D_{50} for all process show similar values.

393 Whatever the process type, the increase of the water content induces expected increases of the
394 apparent median diameter (Fig. 7), with lower contents of the small agglomerates and higher
395 contents of the large agglomerates (Fig. 5-6). The content of the medium agglomerates is the
396 highest at 40% water content. Increasing the water content (from 30 to 50%) does not affect
397 the apparent diameter span values for the reverse processes (Fig. 7).

398 Large differences in the size distribution curves (Fig. 4-5) and in the apparent span values
399 (Fig. 7) of the wet agglomerates have been found for the low water contents (30 or 40%). For
400 the experiments conducted at 50% water content, only slight differences in the particles size
401 distribution curves (Fig. 4C) and the apparent span values (Fig. 7) were demonstrated
402 between the direct process and the reverse processes. There is a low impact of the process on

403 the properties of the agglomerates, when the water content is close to the plastic limit and to
404 the formation of continuous dough.

405

406 3.2.2. Water content distribution

407 As showed by Barkouti el al. (2014) for the direct agglomeration, the results demonstrate
408 whatever the process a significant dispersion of the measured values of the water content
409 between the four classes of the agglomerates, defined by their size (Fig. 8): the large
410 agglomerates are more wet than the small ones, whatever the process water content (30, 40, or
411 50%).

412 Increasing the process water content (from 30 to 50%) significantly increases of the measured
413 water content for the agglomerates of medium size ($0.4 \text{ mm} < d < 1.250 \text{ mm}$), but does not
414 affect the water content of the small and of the large agglomerates.

415 For the reverse plastic process, we observe a lower dispersion of the measured water contents
416 between the four classes of agglomerates (Fig. 8B), compared to the direct process (Fig. 8A).
417 For the reverse liquid process, we observe the higher dispersion of the measured water
418 contents between the four classes of agglomerates (Fig. 8C), close to those of the direct
419 process.

420

421 3.2.3. Compactness distribution

422 Whatever the process, the results demonstrate a significant dispersion of the measured values
423 of the compactness between the four classes of the agglomerates, defined by their size (Fig. 9-
424 10): the large agglomerates are less compact than the small ones, whatever the process water
425 content. Compactness of the agglomerates is linked to their water content, in the same way
426 that Barkouti et al. (2014) have showed.

427 The agglomerates produced by the reverse plastic process are characterized by slightly higher
428 and less dispersed values of the compactness, compared to the direct process. The
429 agglomerates produced by the reverse liquid process are characterized by slightly higher and
430 more dispersed values of the compactness, compared to the direct process. This difference is
431 certainly due to the difference between the agglomeration mechanisms. A potential future
432 work conducted at the particle scale could provide relevant data to describe the impact of the
433 reverse agglomeration process on the compactness values.

434 Increasing the process water content (from 30 to 50%) decreases the compactness values of
435 the wet agglomerates, but does not significantly affect the dispersion of the compactness
436 values.

437

438 3.2.4. Rheological properties

439 The cohesion and the friction coefficient were only measured for the selected wet
440 agglomerates (*i.e.* with size between 1.25 and 2 mm). The reverse processes (plastic or liquid)
441 give the agglomerates with higher values of the friction coefficient and lower values of the
442 cohesion, when compared with the direct process (Fig. 11). Whatever the process, the
443 cohesion of the bed of the wet agglomerates increases with the process water content. We did
444 not observe significant effects of the process water content on the friction coefficient. Similar
445 increase in the cohesion of wheat semolina dough with increasing water contents was
446 observed and discussed by Rondet et al. (2013).

447

448 **3.4. Properties of the dried agglomerates**

449 The dried agglomerates were obtained after the stages of steaming and drying of the selected
450 wet agglomerates (*i.e.* between 1.25 and 2 mm).

451

452 3.4.1. Microstructural description

453 The topology of the surface of the dried agglomerates was described from scanning electron
454 microscopy (Fig. 12). The process significantly affects the superficial microstructure of the
455 agglomerates. The agglomerates produced by the direct process (Fig. 12A) are characterized
456 by more or less spherical shapes, with some irregularities on their surfaces. They are not
457 dense objects, since an apparent porosity opening on the surface is observed. At the low water
458 content, the surface of the agglomerates is made of small particles that seem to be glued to
459 each other but still remained discernible. The increase of the water content during process
460 gives the dried agglomerates with smooth areas on their surface. It is difficult to identify the
461 native particles, because they are partly melted and merged, due to the specific reactivity of
462 the hydrated wheat proteins which composes the semolina particles.

463 The agglomerates produced by the reverse processes (Fig. 12B-C) are characterized with
464 heterogeneous and shapes far from sphere. When processed at low water content (30%) by the
465 reverse processes, the agglomerates are characterized by lengthened shapes. The surface of
466 the agglomerates is made by an apparent continuous medium, with some visible small
467 particles glued, giving the aspect of granular roughness. The proportion of the small particles
468 is higher on surface of the agglomerates produced by the reverse plastic process, when
469 compared to those produced by the reverse liquid process.

470 When processed at intermediary water content (40%) by the reverse processes, the
471 agglomerates are characterized by original flat shapes, comparable to glitters or flakes. The
472 shape ratio (i.e. apparent thickness / diameter) is estimated at 1/5. The surface of these
473 agglomerates is made by the association of particles, which seems to be glued on each other.

474 When processed at high water content (50%) by the reverse processes, the agglomerates are
475 characterized by heterogeneous and not spherical shapes. The surface of the agglomerates is
476 then made by smooth areas on which some particles are merged. The proportion of the
477 merged particles is lower on the agglomerates produced by the reverse plastic process, than
478 on those produced by the reverse liquid process.

479

480 3.4.2. Compactness

481 Whatever the process water content of the wet agglomerates, the compactness of the dried
482 agglomerates produced by the reverse plastic process (0.841) or by the reverse liquid process
483 (0.848) are slightly higher than those produced by the direct process (0.831) (Fig. 13). We do
484 not identify significant effect of the process water content on the values of compactness for
485 the dried agglomerates.

486

487 3.4.3. Colour properties

488 The colour characteristics of dried agglomerates produced by the reverse processes are
489 significantly different to those produced by the direct process (Fig. 13). The colour difference
490 with wheat semolina (ΔE) is close to 36.8 for the agglomerates produced by the direct
491 process. The reverse plastic process produced agglomerates with lower values of colour
492 difference ($\Delta E = 33.4$), due to specific values of the brightness (L^*). For the reverse liquid
493 process, the colour difference ($\Delta E = 35.9$) is close to those of the direct process.

494

495 3.4.4. Swelling properties

496 The process influences the swelling ability of the agglomerates (Fig. 13). The swelling
497 capacity of the dried agglomerates describes their ability to interact with water molecules,
498 which depends on the crystalline state of the starch granules, and on the ability of the porous
499 agglomerates to swell and entrap water inside the internal voids (Cuq et al., 2013).

500 The swelling capacity of the dried agglomerates produced by the reverse plastic or liquid
501 process (3.10 or 3.08 mL.g⁻¹) are slightly higher than those measured for the direct process
502 (2.95 mL.g⁻¹). Whatever the process, the increases in the process water content of the wet
503 agglomerates before the stage of steaming increase their swelling capacity after the drying.

504 Higher water contents of the wet agglomerates enhance the mechanisms of gelatinization of
505 the starch granules during the steaming stage, the loss of the crystalline structures, and the
506 formation of amorphous hygroscopic structures in the dried agglomerates.

507

508 **4. DISCUSSION**

509 The major aim of this work was to investigate the performance of an original new reverse
510 agglomeration process (based on the fragmentation of a dough and the formation of
511 agglomerates, by adding a dry powder), in comparison with the direct wet agglomeration
512 process: water droplets on particles, or the novel reverse-phase wet granulation process:
513 particles in water layer (Wade et al., 2014).

514

515 During the reverse agglomeration process, the first stage of the elaboration of the continuous
516 dough is conducted to initiate **physicochemical mechanisms** based on the reactivity of the
517 wheat components under high water contents and mechanical shear stresses. These
518 mechanisms generate irreversible changes of the wheat components (solubilization of proteins
519 and fibers, formation of protein network) inside the dough (Bloksma 1990, Eliasson 1990,).
520 Two conditions of dough water contents were investigated to modulate the extent of the
521 physicochemical mechanisms: the reserve plastic process at 75% water content, with the
522 dough of high consistency and low reactivity; the reverse liquid process at 110% water
523 content, with the dough of low consistency and high reactivity.

524

525 The present study allows investigating the apparent electric cost of the physicochemical
526 mechanisms during the process, and more particularly during the period of mixing of the
527 continuous dough and of the fragmentation stage. Compared to the direct process, the electric
528 cost of the reverse process is almost similar when considering the liquid dough conditions
529 (Table 2). The low consistency of the liquid dough does not require overconsumption of the
530 electric power in order to be mixed. The high molecular reactivity under the liquid dough
531 conditions does not generate electric overcosts during the agglomeration process. The electric
532 costs of the mixing of the continuous dough of low consistency are close to those of the
533 mixing of the granular paste in the classic agglomeration process. On the other hand, the
534 electric cost is higher when considering the plastic dough. The high consistency of the plastic
535 dough requires electric overconsumption during the stage of mixing.

536 The energy cost of the reverse agglomeration process is thus not proportional to the extent of
537 physicochemical mechanisms involving the wheat components. The reverse agglomeration
538 process can thus be managed to promote different irreversible physicochemical reactions
539 without negative impacts on the electric energy costs.

540

541 The present work demonstrates that the **characteristics** of the continuous dough are important
542 factors during the reverse agglomeration process, because they directly contribute to the
543 physical mechanisms involved in the formation of the agglomerates. They impact more
544 particularly the relative dispersion of the individual properties of the agglomerates.

545 (i) The low consistency of the liquid dough is favourable to the mixing efficiency of
546 the mixer, in order to quickly generate homogeneous dough at the end of the initial stage of
547 the addition of water. On the other hand when considering the plastic dough with the high
548 consistency, more process time is required during the initial stage of mixing in order to obtain
549 a homogeneous dough.

550 However, the present results do not demonstrate the lower dispersion of the individual
551 properties of the agglomerates produced by the liquid reverse process, when compared with
552 the reverse plastic dough process (Fig. 8-9). The capability of the mixer to homogenize the
553 dough thus does not seem to affect the dispersion of the individual properties of the
554 agglomerates.

555 (ii) The final stage of the addition of power during the reverse process is conducted in
556 order to promote the **controlled breakage mechanisms** of the continuous dough. The
557 breakage mechanisms are generated by adding the native particles under mechanical stresses
558 to produce the wet agglomerates. The wet agglomerates are made by the association of small
559 pieces of dough and of the dry native particles. It should be pointed out that the spans of size
560 distributions obtained by using the reverse process are narrower than that obtained for direct
561 agglomeration process. The breakage mechanisms during the reverse process are thus not less
562 efficient in order to produce grains with homogeneous characteristics, compared to the growth
563 mechanisms during the direct process. The reverse process makes it possible to increase the
564 agglomeration yields of the process. Wade et al. (2014, 2015) also indicated that size
565 distribution of the granules may be simpler to be controlled in the reverse-phase granulation
566 process. The size of the granules progressed towards a unimodal distribution indicating that
567 improved mechanical dispersion occurred.

568

569 The present work demonstrates that the ability of the continuous dough to be fragmented in
570 small pieces is partly dependent on the characteristics of the dough. The low consistency of
571 the liquid dough is favourable to the dispersed mechanisms of breakage: this allows the
572 formation of pieces of dough, with high dispersion in the sizes and properties (Fig. 8-9). On
573 the other hand, the high consistency of the plastic dough requires more energy for the
574 breakage mechanisms: the high cohesion of the dough favours the effects of mixing and
575 allows the formation of homogeneous pieces of dough, with low dispersion in the size and
576 properties, such as water content or compactness.

577
578 Strong differences in the **microstructure** of the agglomerates were demonstrated when
579 comparing the direct and reverse processes (Fig. 12). The direct process generated classical
580 round to ellipsoid structures. The reverse processes generate particles with no spherical
581 shapes, but with original shape close to the flakes. Our results, show different trends when
582 compared to Rondet (2008) who found that the reverse agglomeration experiments produced
583 "more spherical and compact (agglomerates) than those produced by the classical wet
584 agglomeration process". These differences could be due to differences in the range of plastic
585 and liquid behaviour of the continuous dough. In addition, their microstructure is
586 heterogeneous due to the fact that native particles at the surface are entrapped in an apparent
587 pasty matrix. This makes it possible to generate composite material with different
588 components. The end use properties can thus significantly differ from those of the
589 agglomerates obtained thanks to the direct process. It makes it possible to consider the
590 prospect of new product development in which the added powder is different from that used
591 to generate the dough.

592
593 The variations of the compactness and water content of the agglomerates during the process
594 can be discussed by using the **hydro-textural diagram** (Ruiz et al., 2005) (Fig. 14). This
595 diagram is limited in its upper part by the saturation curve, which represents the maximum
596 water content that a medium of a given compactness can contain. Whatever the process, the
597 increase in agglomerates size is concomitant with an increase in their water content and a
598 decrease of their compactness. The results are similar to those obtained thanks to a classical
599 agglomeration process, in the conditions of wetting and mixing which corresponding to the
600 drop control regime of nucleation (Rondet et al., 2010). Nevertheless, the agglomerates
601 generated in this study (and whatever the process chosen) are found to be totally saturated
602 with water (Fig. 14). In the case of the reverse process, this result is not surprising insofar the

603 agglomerates are generated from initially saturated dough pieces. When the direct
604 agglomeration process is considered, the saturation of agglomerates is dependent on the
605 conditions of wetting and mixing, that impose a mechanical dispersion regime of nucleation.
606 Wade et al. (2014) have demonstrated that the reverse-phase process is able to generate
607 granules with low intragranular porosity when starting from dense suspension, due to the
608 complete filling of intraparticulate pores by the binder liquid in the initial phases of the
609 process. The addition of further powders reduces the liquid saturation of the granules, with the
610 desired particle size being obtained through controlled breakage. Proposed advantages of the
611 reverse-phase process over the conventional wet granulation approach include a reduced risk
612 of uncontrolled granule growth. Wade et al. (2015) have indicated that the conventional
613 process showed granule growth driven by viscous forces, whereas the reverse-phase process
614 showed granule breakage driven by capillary forces.

615

616 **5. CONCLUSION**

617 The different agglomeration processes have been found to generate agglomerates with
618 specific functional attributes, due to the physicochemical reactivity of the wheat semolina
619 components. Dough characteristics and fragmentation mechanisms have been found to
620 contribute to the determinism of the end use properties of the agglomerates. The multiplicity
621 of mechanisms and interactions identified during the reverse agglomeration of the durum
622 wheat semolina offers the opportunity to generate diversity of the agglomerates. The
623 relationship between the process parameters and the end use properties of the resulting
624 agglomerates still needs to be better understood, for instance by investigating the spatial
625 distribution of the mechanisms at a local scale, inside the structure of the agglomerates. This
626 work offers innovative potentials to design the reverse agglomeration process for food
627 powders and generate news products.

628

629 **Acknowledgments**

630 The authors sincerely acknowledge Miss Macarena Soledad Silva Castro for her significant
631 contribution in the experimental work.

632

633 **REFERENCES**

634

635 Abecassis J., Cuq B., Boggini G., and Namoune H., 2012. Other traditional durum derived
636 products. In *Durum Wheat: Chemistry and Technology*, 2nd ed. M.J. Sissons, J. Abecassis, B.
637 Marchylo, and M. Carcea (Eds.), AACC International, pp 177-200.

638

639 AFNOR V 03-050, 1970. Norme française, Directives générales pour le dosage de l'azote
640 avec minéralisation selon la méthode de Kjeldahl.

641

642 AFNOR P 94-051, 1993. Norme française. Détermination des limites d'Atterberg. Limite de
643 plasticité au rouleau.

644

645 AFNOR P 94-052-1, 1995. Norme française. Détermination des limites d'Atterberg. Limite
646 de liquidité. Méthode du cône de pénétration.

647

648 AACC, 2000. American Association of Cereal Chemists. Official Methods of the AACC, 10th
649 ed. Method 76-13, First approval November 8, 1995; Reapproval November 3, 1999. The
650 Association: St. Paul, MN, USA.

651

652 Barkouti A., Delalonde M., Rondet E., Ruiz T., 2014, Structuration of wheat powder by wet
653 agglomeration: Case of size association mechanism. *Powder Technol.* 252, 8-13.

654

655 Bloksma, A.H. 1990. Dough structure, dough rheology, and baking quality. *Cereal Foods*
656 *World* 35: 237-244.

657

658 Cuq, B., Mandato, S., Jeantet, R., Saleh, K., Ruiz, T., 2013. Food powder agglomeration. In
659 *Handbook of Food Powders*. B. Bhandari, N. Bansal, M. Zhang, and P. Schuck, (Eds.),
660 Woodhead Publishing Series in Food Science, Technology and Nutrition No. 255, pp. 150-
661 177.

662

663 Eliasson, A.C., 1990. Rheological properties of cereal proteins. In *Dough Rheology and*
664 *Baked Product Texture*. H. Faridi and J.M. Faubion (Eds.), Van Nostrand Reinhold, New
665 York, NY, pp. 67-110.

666

- 667 Ennis, B.J., Tardos, G.I., Pfeffer, R., 1991. A microlevel-based characterization of granulation
668 phenomena, *Powder Technol.* 65, 257-272.
- 669
- 670 Guezlane, L., Abecassis, J., 1991. Methodes d'appréciation de la qualite culinaire du couscous
671 de blé dur. *Industries Alimentaires et Agricoles*, 108, 966-971.
- 672
- 673 Hapgood, K., Litster, J.D., Smith, R., 2003. Nucleation regime map for liquid bound granules.
674 *AIChE Journal* 49, 350-361.
- 675
- 676 Holtz, R.D., Kovacs, W.D., 1981. An introduction to geotechnical engineering, Prentice-Hall,
677 Inc., Englewood Englewood Cliffs, N.J., USA.
- 678
- 679 Iveson, S.M., Litster, J.D., Hapgood, K., Ennis, B.J., 2001. Nucleation, growth and breakage
680 phenomena in wet granulation processes : a review. *Powder Technol.* 117, 3-39.
- 681
- 682 Li, B., Reynolds, T.D., Mukai, R.G., 2010. Granulates, process for preparing them and
683 pharmaceutical products containing them. International Patent, WO 2010/033179 A1.
- 684
- 685 Litster, J.D., Ennis, B.J., 2004. The science and engineering of granulation processes,
686 Dordrecht, Kluwer Powder Technology Series.
- 687
- 688 Mandato, S., Rondet, E., Delaplace, G., Barkouti, A., Galet, L., Accart, P., Ruiz, T., Cuq, B.,
689 2012. Liquids' atomization with two different nozzles: Modeling of the effects of some
690 processing and formulation conditions by dimensional analysis. *Powder Technol.* 224, 323-
691 330.
- 692
- 693 Palzer, S., 2011. Agglomeration of pharmaceutical, detergent, chemical and food powders -
694 Similarities and differences of materials and processes. *Powder Technol.* 206, 2-17.
- 695
- 696 Pollini, C.M., Pantò, F., Nespoli, A., Sissons, M., and Abecassis, J., 2012. Manufacture of
697 pasta products. In *Durum Wheat: Chemistry and Technology*, 2nd ed., M.J. Sissons, J.
698 Abecassis, B. Marchylo, and M. Carcea (Eds.), p 161-176, AACC International.
- 699

- 700 Reynolds, G.K., Fu, J.S., Cheong, Y.S., Hounslow, M.J., Salman, A.D., 2005. Breakage in
701 granulation: A review. *Chem. Eng. Sci.* 60, 3969-3992.
702
- 703 Rondet, E., 2008. Capillary texturation of humid granular media. PhD Thesis, Université
704 Montpellier II, France.
705
- 706 Rondet, E., Delalonde, M., Ruiz, T., Desfours, J.P., 2010. Fractal formation description of
707 agglomeration in low shear mixer. *Chem. Eng. J.* 164, 376-382.
708
- 709 Rondet, E., Denavaut, M., Mandato, S., Duri, A., Ruiz, T., Cuq, B., 2012. Power consumption
710 profile analysis during wet agglomeration process: Energy approach of wheat powder
711 agglomeration. *Powder Technol.* 229, 214-221.
712
- 713 Rondet, E., Ruiz, T., Cuq, B., 2013. Rheological and mechanical characterization of wet
714 agglomerates processed in low shear mixer. *J. Food Eng.* 117, 67-73.
715
- 716 Ruiz, T., Delalonde, M., Bataille, B., Baylac, G., Dupuy de Crescenzo, C., 2005. Texturing
717 unsaturated granular media submitted to compaction and kneading processes. *Powder
718 Technol.* 154, 43-53.
719
- 720 Saleh, K., Guigon, P., 2009. Mise en œuvre des poudres. *Techniques de granulation humide et
721 liants, Techniques de l'ingénieur*, J2 253, 1-14.
722
- 723 Wade, J., Martin, G.P., Long, D.F., 2013. Development of a growth regime map for a novel
724 reverse phase wet granulation process. Poster presented at the 6th International Granulation
725 Workshop (26-28th June, Sheffield, England).
726
- 727 Wade, J.B., Martin, G.P., Long, D.F., 2014. Feasibility assessment for a novel reverse-phase
728 wet granulation process: the effect of liquid saturation and binder liquid viscosity. *Int. J.
729 Pharm.* 475, 450-461.
730
- 731 Wade, J.B., Martin, G.P., Long, D.F., 2015. Controlling granule size through breakage in a
732 novel reverse-phase wet granulation process; the effect of impeller speed and binder liquid
733 viscosity. *Int. J. Pharm.* 478, 439-446.

Figure 1: Schematic description of the three investigated agglomeration processes, direct process (A), reverse plastic process (B), or reverse liquid process (C), as a function of the process water content.

Figure 2: Schematic description of the successive stages during the three investigated agglomeration processes: direct process (A) or reverse processes (B).

Figure 3: Typical normalized electric input power curves monitored during the agglomeration of wet agglomerates at 30% water content. With the direct agglomeration process (A), the reverse plastic process (B), and the reverse liquid process (C).

Figure 4: Impact of the agglomeration process (direct process, reverse plastic process, or reverse liquid process), and of the process water content (at 30% (A), 40% (B), or 50% (C) water content), on the measured particle size distribution curves of the wet agglomerates.

Figure 5: Impact of the process water content (at 30, 40, or 50%) and of the agglomeration process (direct (A), reverse plastic (B), or reverse liquid (C) process) on the measured particle size distribution curves of the wet agglomerates.

Figure 6: Mass proportion for the 4 classes of the wet agglomerates, as a function of the process water content (at 30, 40, or 50%) and the process type: direct process (A), reverse plastic process (B), or reverse liquid process (C).

Figure 7: Impact of the process water content on the apparent median diameter (d_{50}) (A) and apparent span diameter dispersion (B) of the wet agglomerates produced by the different processes.

Figure 8: Water content values for the 4 different classes of the wet agglomerates, as a function of the process water content (at 30, 40, or 50%) and the process type: direct process (A), reverse plastic process (B), or reverse liquid process (C).

Figure 9: Compactness values for the 4 classes of the wet agglomerates, as a function of the process water content (at 30, 40, or 50%) and the process type: direct process (A), reverse plastic process (B), or reverse liquid process (C).

Figure 10: Impact of the process water content on the compactness of the selected wet agglomerates ($1.25 < \text{diameter} < 2 \text{ mm}$), produced by the different processes.

Figure 11: Impact of the process water content on the rheological properties (cohesion and friction coefficient) of the selected wet agglomerates ($1.25 < \text{diameter} < 2 \text{ mm}$) produced by the different processes.

Figure 12: Microstructure by SEM of the dried agglomerates produced by the different process (direct, reverse plastic, or reverse liquid process) at the different process water content (at 30, 40, or 50%).

Figure 13: Impact of the process water content on the properties (compactness, color characteristics and the swelling properties) of the dried agglomerates, produced by the different processes.

Figure 14: Hydro-textural description (compactness vs. measured water content) of the wet agglomerates and of the dried agglomerates, produced by the different processes (direct, reverse plastic, or reverse liquid processes).

Table 1: Description of the experimental conditions (initial load of powder, mass of added water, and mass of added powder) defined for the successive stages of the agglomeration processes at the different process water content.

	Process water content (% db)	Initial load of powder (g)	Mass of added water (g)	Mass of added powder (g)	Total final Load (g)
Direct	30	1347	153	--	1500
	40	1250	250	--	1500
	50	1167	333	--	1500
Reverse (75%)	30	307	154	1039	1500
	40	500	250	750	1500
	50	667	333	500	1500
Reverse (110%)	30	191	153	1156	1500
	40	314	252	934	1500
	50	417	333	750	1500

Table 2: Mechanical energy consumption (kJ) measured during the successive stages of the agglomeration processes at the different process water content.

	Process		Mechanical energy consumption (kJ)			
	water content (% db)	Process	Total	Initial load	Water addition	Fragmen-tation
			Process	mixing	stage	stage
Direct	30	11.3 (± 0.6) ^a	0.76 (± 0.07) ^e	10.4 (± 0.9) ^{de}	-	
	40	12.9 (± 0.8) ^b	0.60 (± 0.05) ^d	12.3 (± 1.2) ^e	-	
	50	27.0 (± 1.6) ^d	0.57 (± 0.06) ^d	26.4 (± 2.4) ^f	-	
Reverse (75%)	30	25.6 (± 1.5) ^d	0.64 (± 0.06) ^{de}	7.2 (± 0.8) ^c	13.1 (± 1.4) ^a	
	40	34.3 (± 2.0) ^e	0.11 (± 0.02) ^b	9.1 (± 1.0) ^d	24.9 (± 2.6) ^b	
	50	60.6 (± 3.5) ^f	0.26 (± 0.03) ^c	10.8 (± 1.0) ^{de}	49.3 (± 5.3) ^d	
Reverse (110%)	30	13.2 (± 0.8) ^b	0.05 (± 0.01) ^a	1.4 (± 0.2) ^a	11.8 (± 1.2) ^a	
	40	16.7 (± 1.0) ^c	0.31 (± 0.03) ^c	3.3 (± 0.4) ^b	13.1 (± 1.4) ^a	
	50	37.7 (± 2.2) ^e	0.07 (± 0.01) ^a	10.2 (± 1.1) ^d	36.6 (± 4.2) ^c	

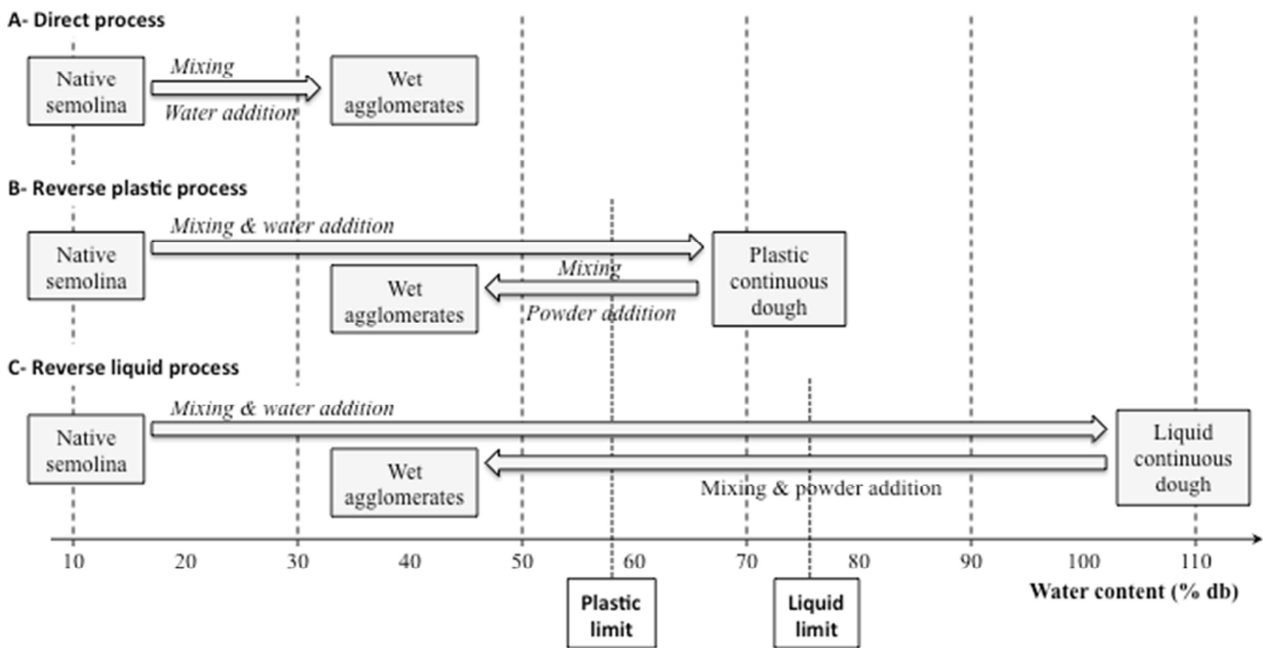


Figure 1: Schematic description of the three investigated agglomeration processes, direct process (A), reverse plastic process (B), or reverse liquid process (C), as a function of the process water content.

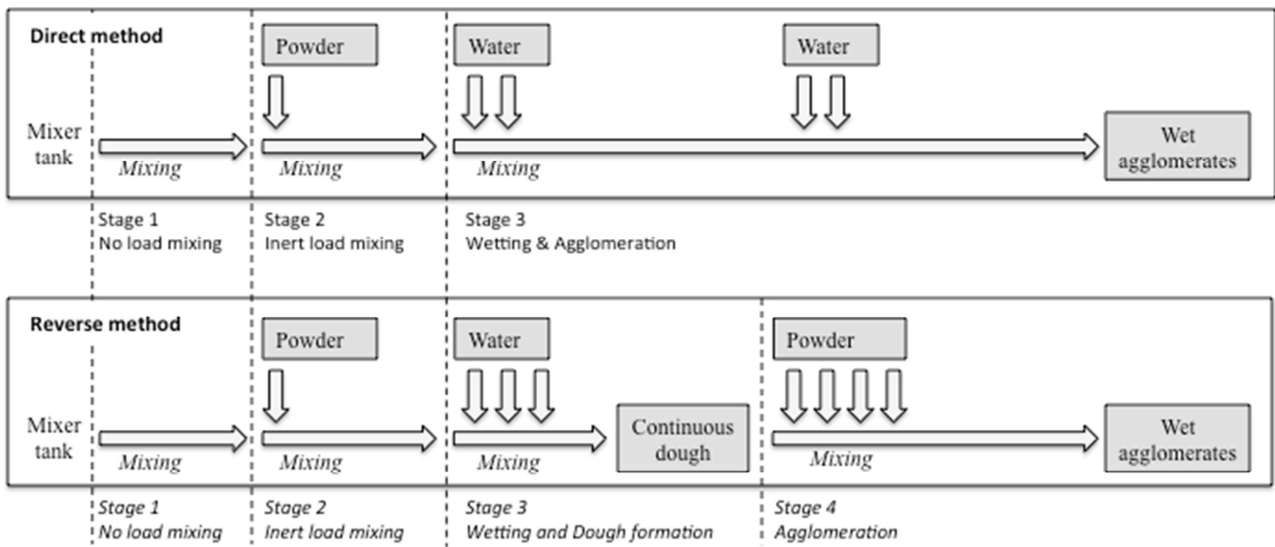


Figure 2: Schematic description of the successive stages during the three investigated agglomeration processes: direct process (A) or reverse processes (B).

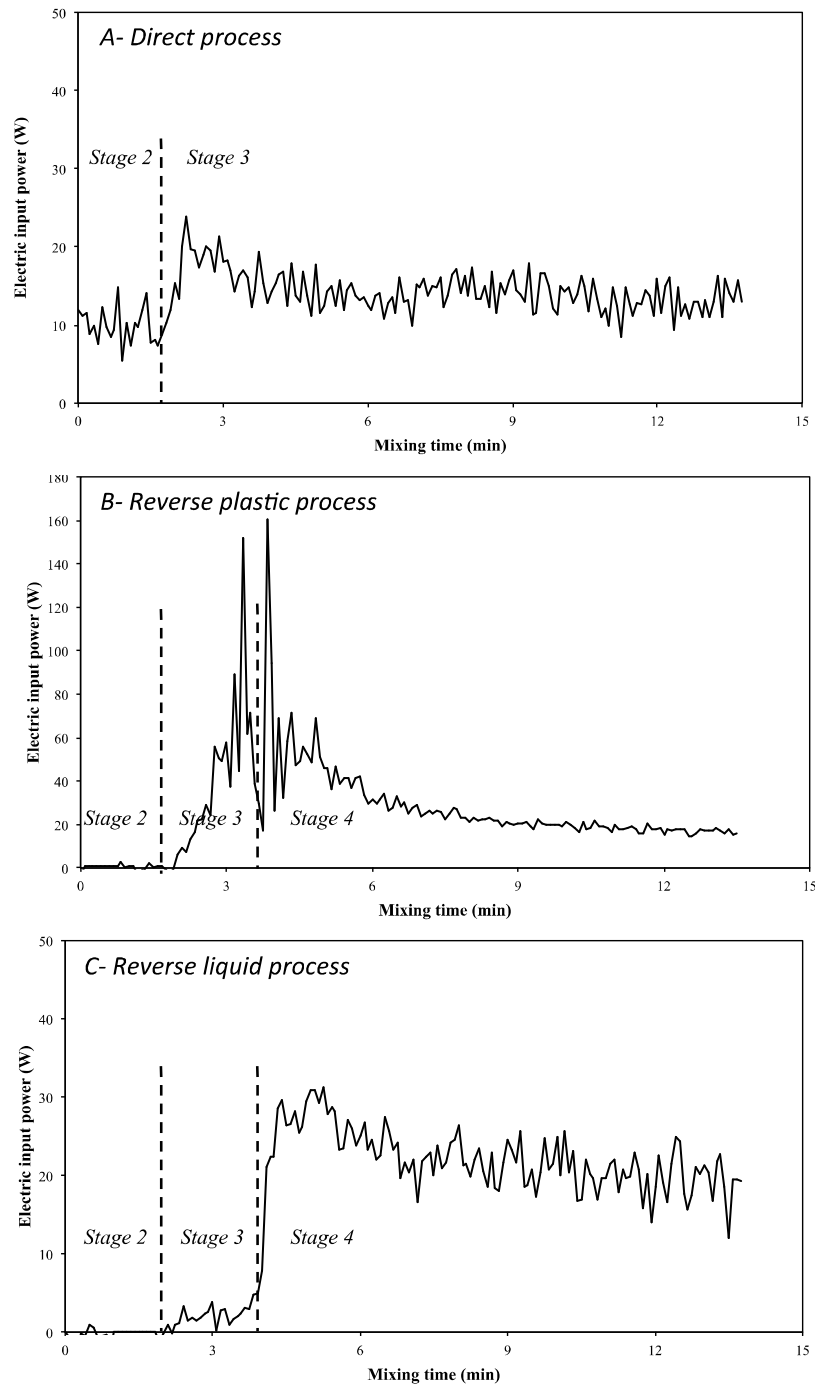


Figure 3: Typical normalized electric input power curves monitored during the agglomeration of wet agglomerates at 30% water content. With the direct agglomeration process (A), the reverse plastic process (B), and the reverse liquid process (C).

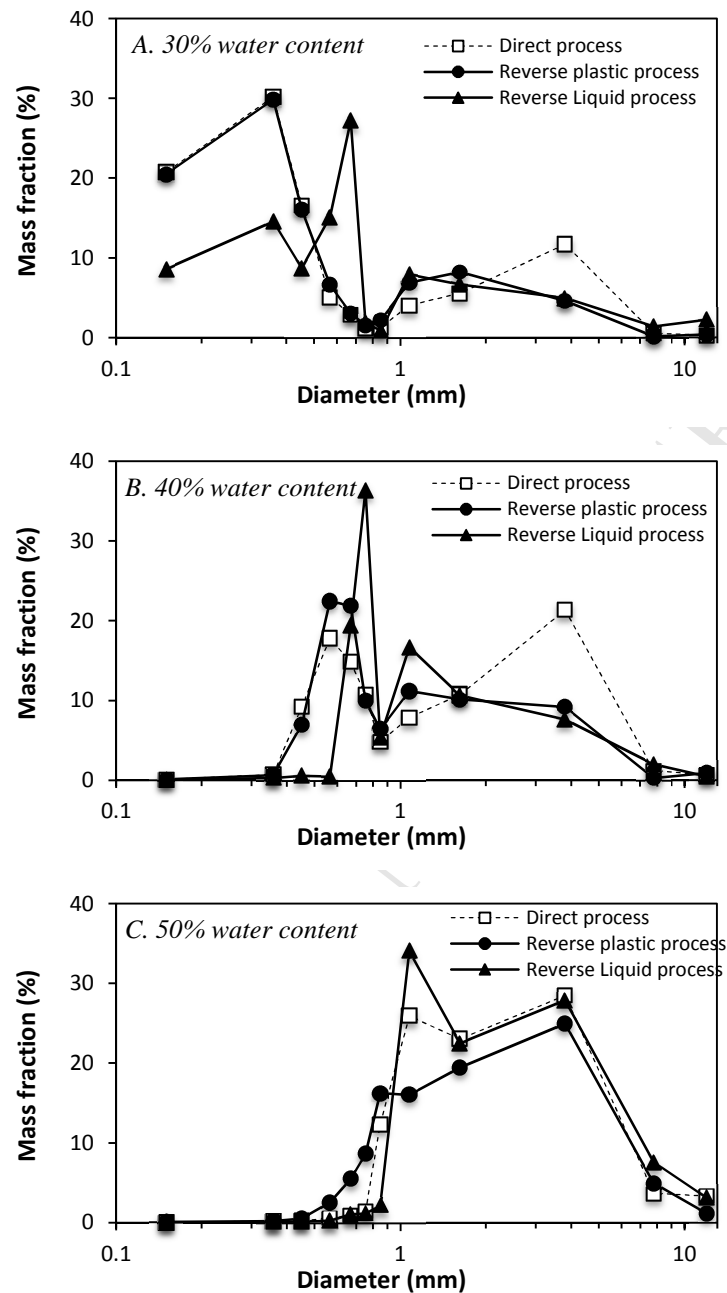


Figure 4: Impact of the agglomeration process (direct process, reverse plastic process, or reverse liquid process), and of the process water content (at 30% (A), 40% (B), or 50% (C) water content), on the measured particle size distribution curves of the wet agglomerates.

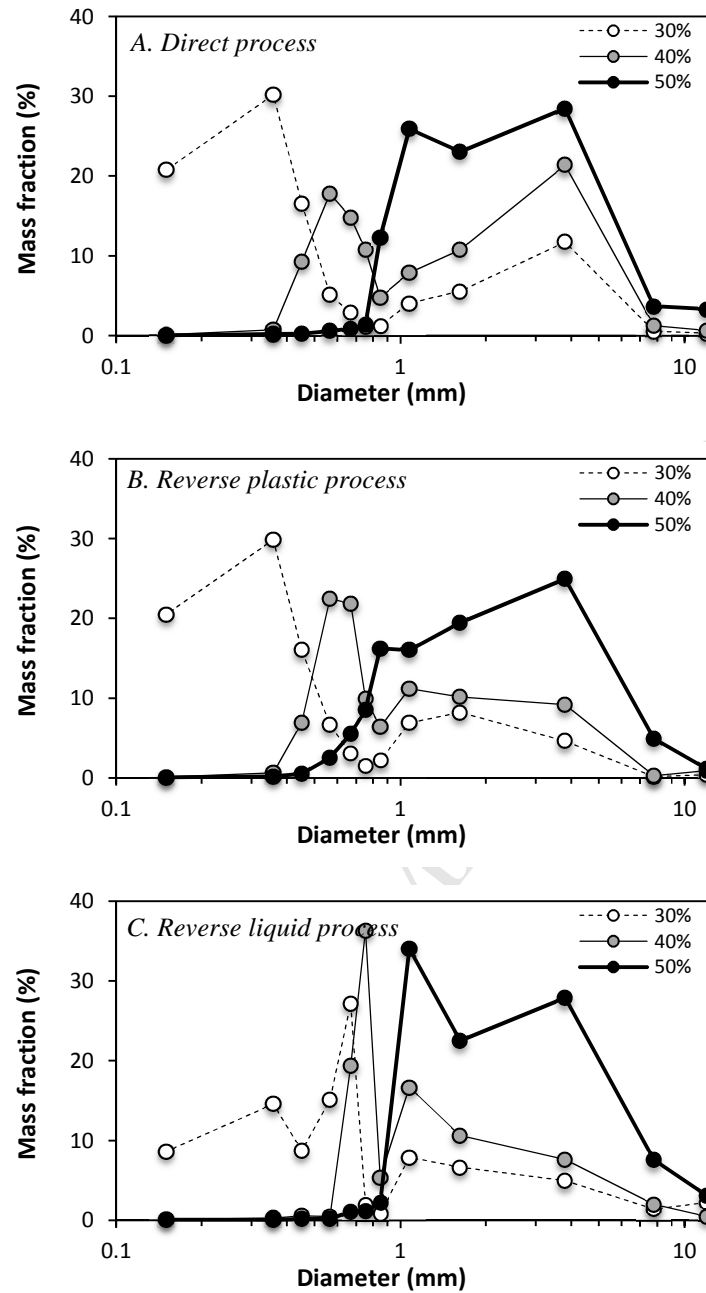


Figure 5: Impact of the process water content (at 30, 40, or 50%) and of the agglomeration process (direct (A), reverse plastic (B), or reverse liquid (C) process) on the measured particle size distribution curves of the wet agglomerates.

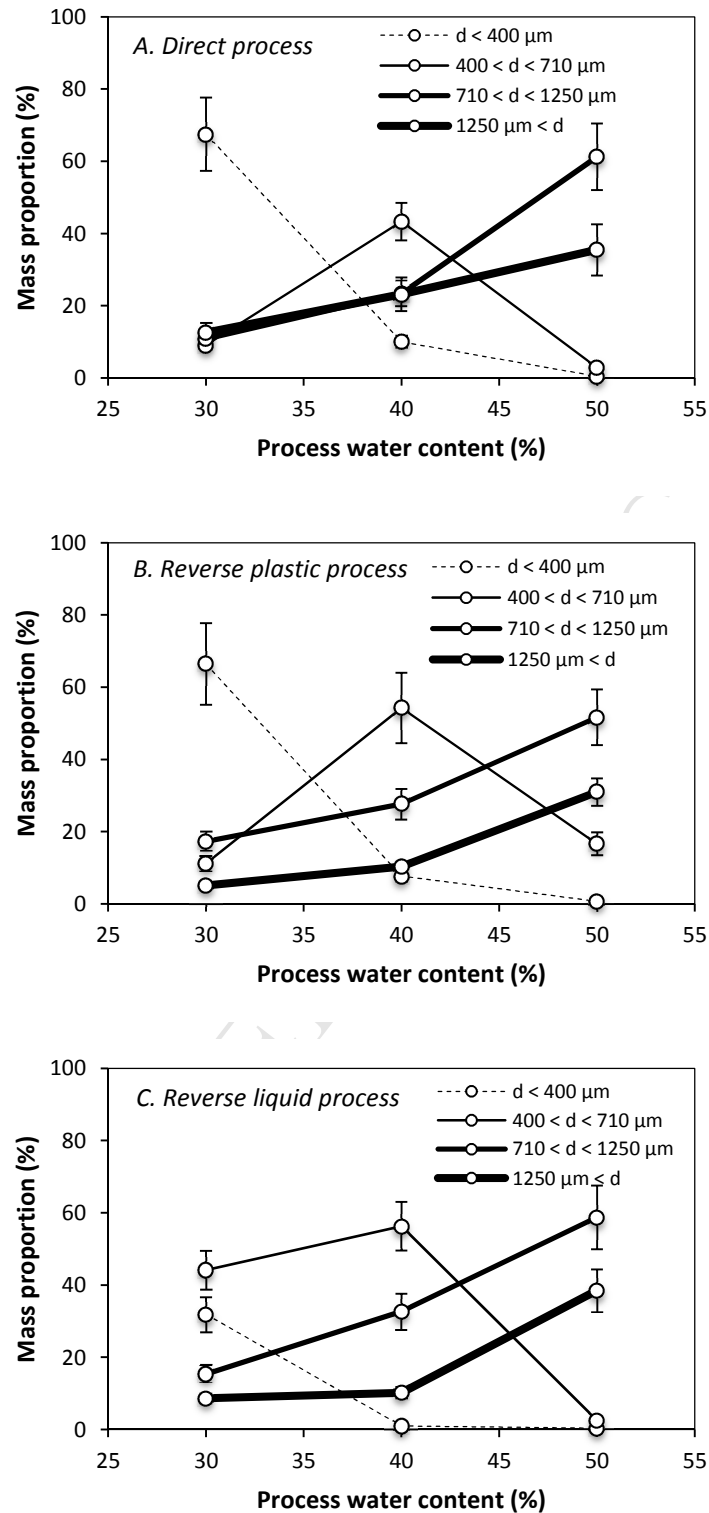


Figure 6: Mass proportion for the 4 classes of the wet agglomerates, as a function of the process water content (at 30, 40, or 50%) and the process type: direct process (A), reverse plastic process (B), or reverse liquid process (C).

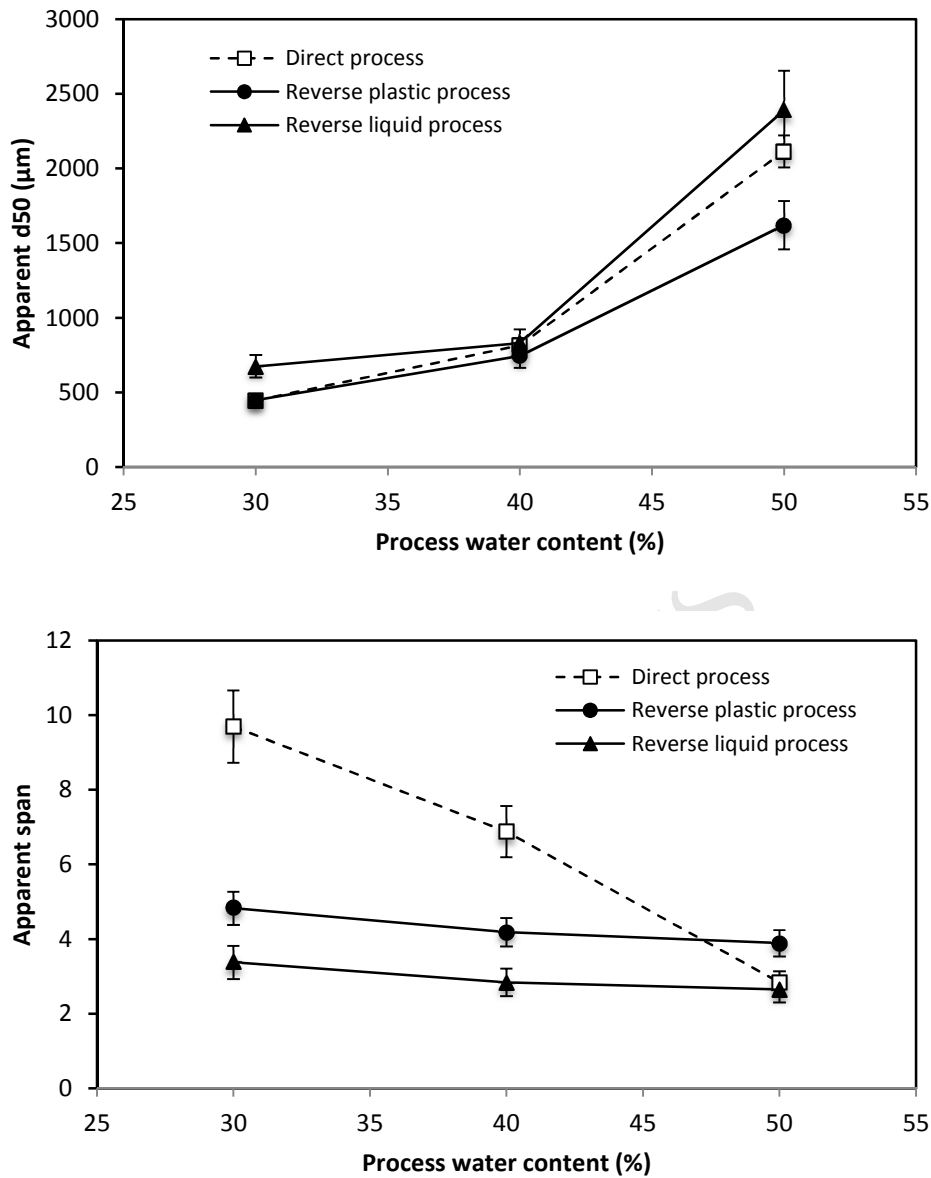


Figure 7: Impact of the process water content on the apparent median diameter (d_{50}) (A) and apparent span diameter dispersion (B) of the wet agglomerates produced by the different processes.

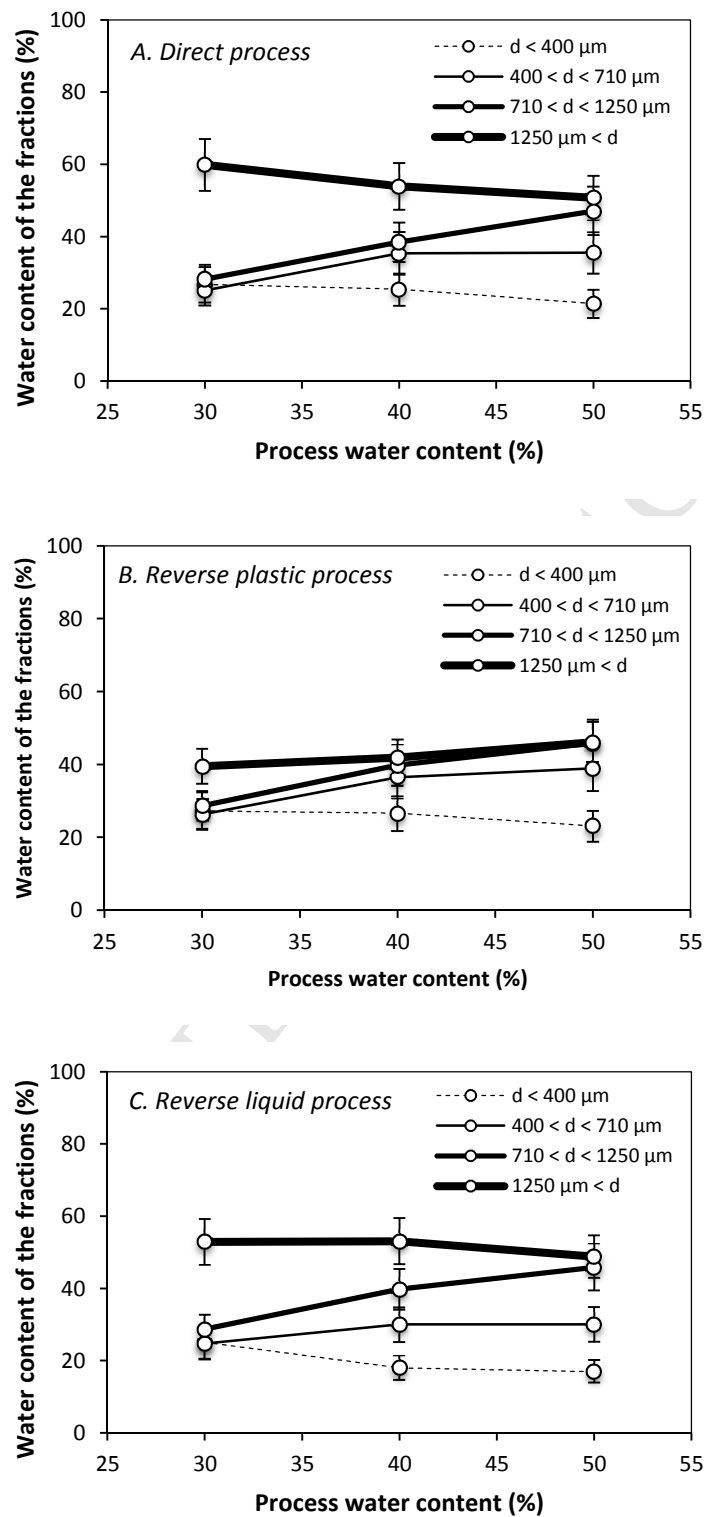


Figure 8: Water content values for the 4 different classes of the wet agglomerates, as a function of the process water content (at 30, 40, or 50%) and the process type: direct process (A), reverse plastic process (B), or reverse liquid process (C).

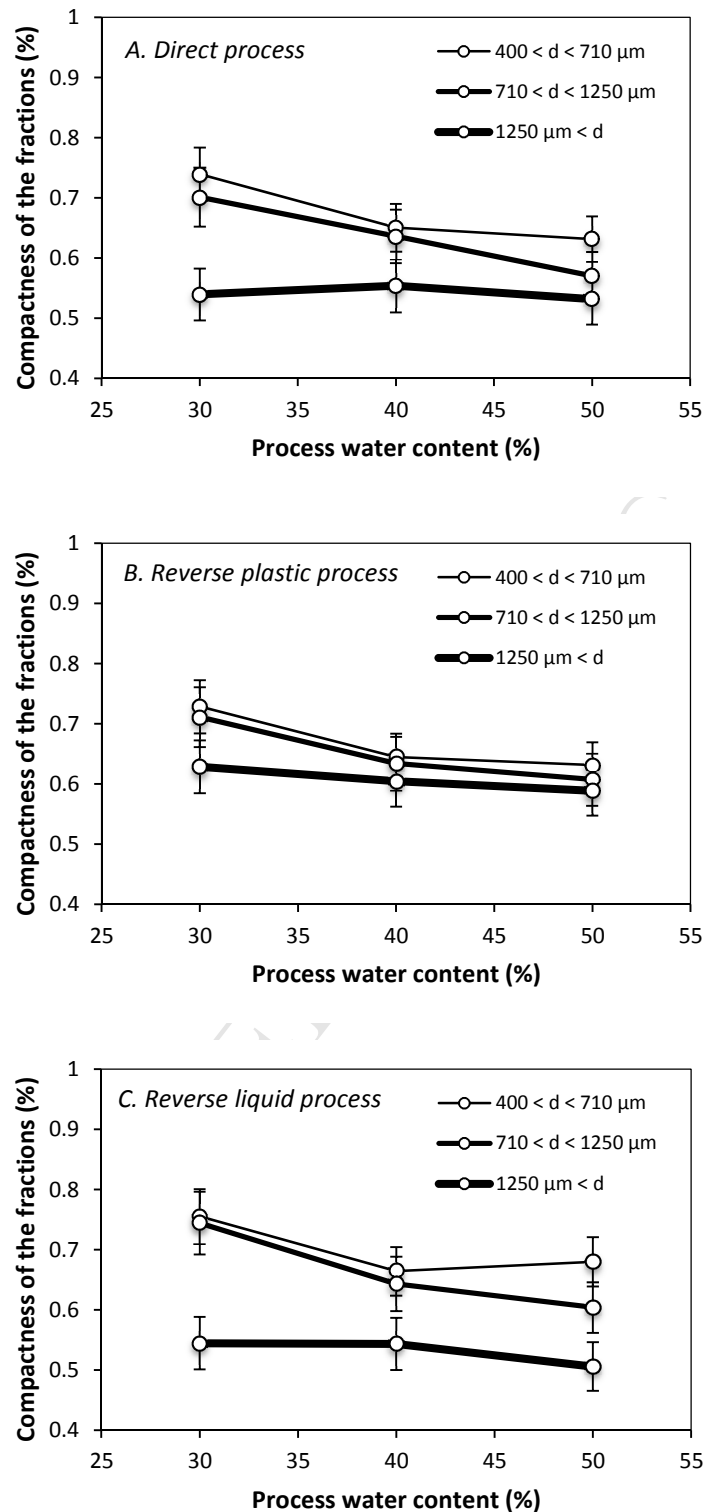


Figure 9: Compactness values for the 4 classes of the wet agglomerates, as a function of the process water content (at 30, 40, or 50%) and the process type: direct process (A), reverse plastic process (B), or reverse liquid process (C).

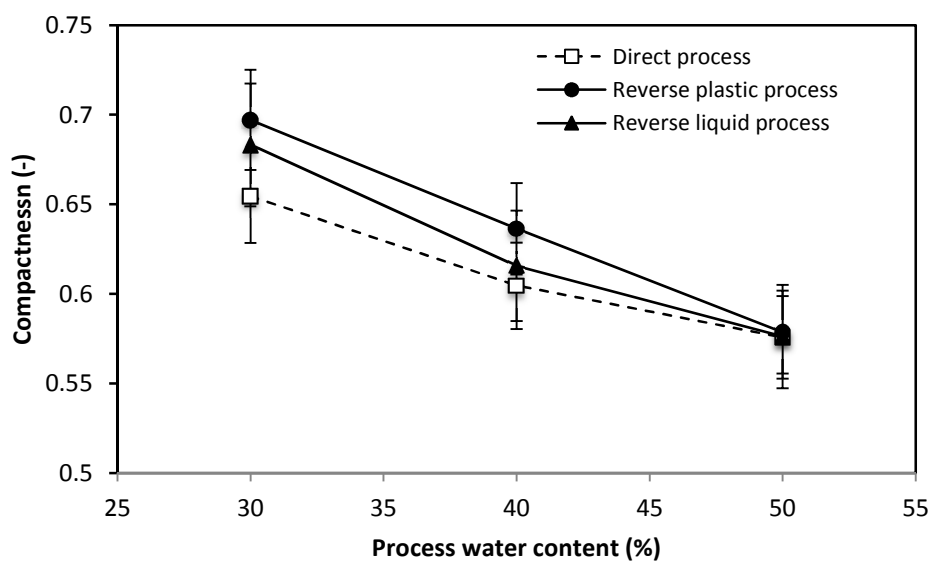


Figure 10: Impact of the process water content on the compactness of the selected wet agglomerates ($1.25 < \text{diameter} < 2 \text{ mm}$), produced by the different processes.

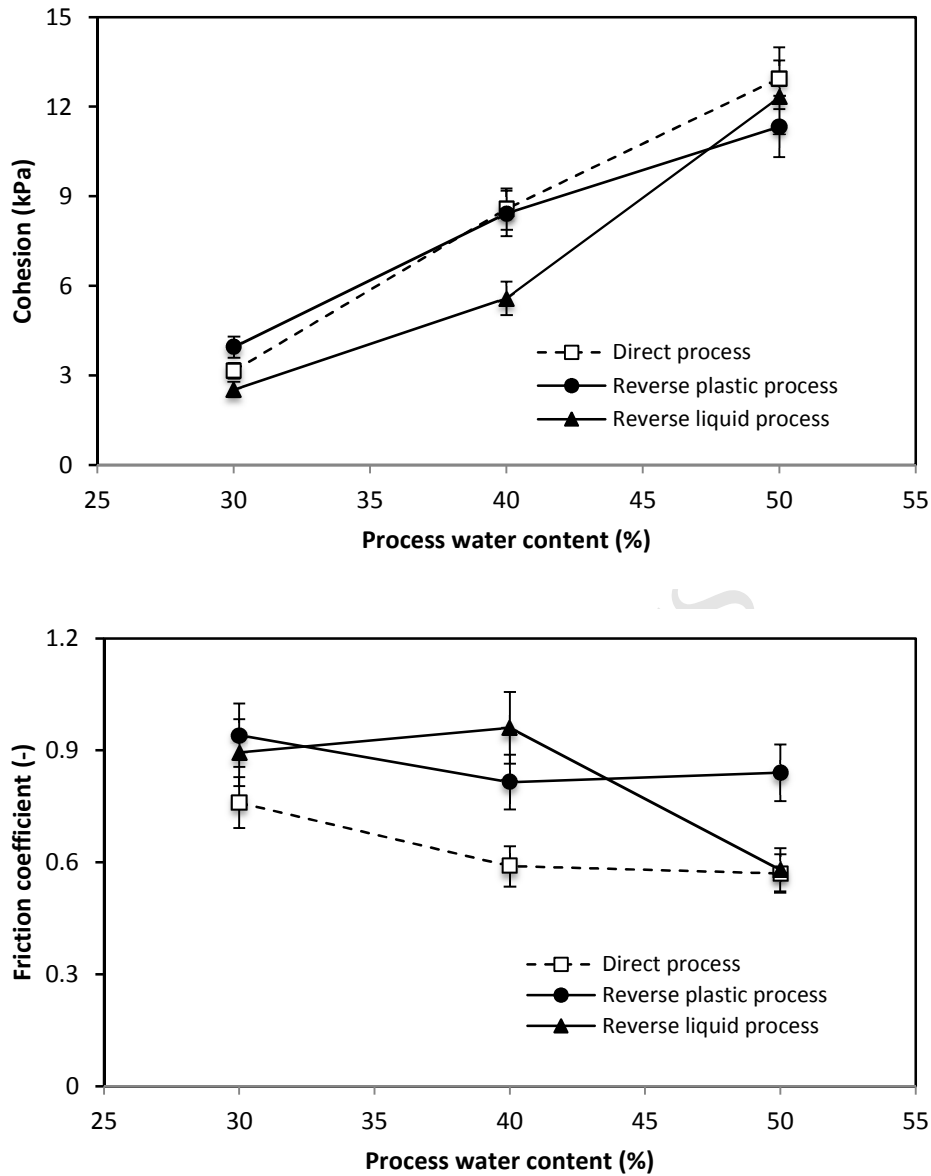


Figure 11: Impact of the process water content on the rheological properties (cohesion and friction coefficient) of the selected wet agglomerates ($1.25 < \text{diameter} < 2$ mm) produced by the different processes.

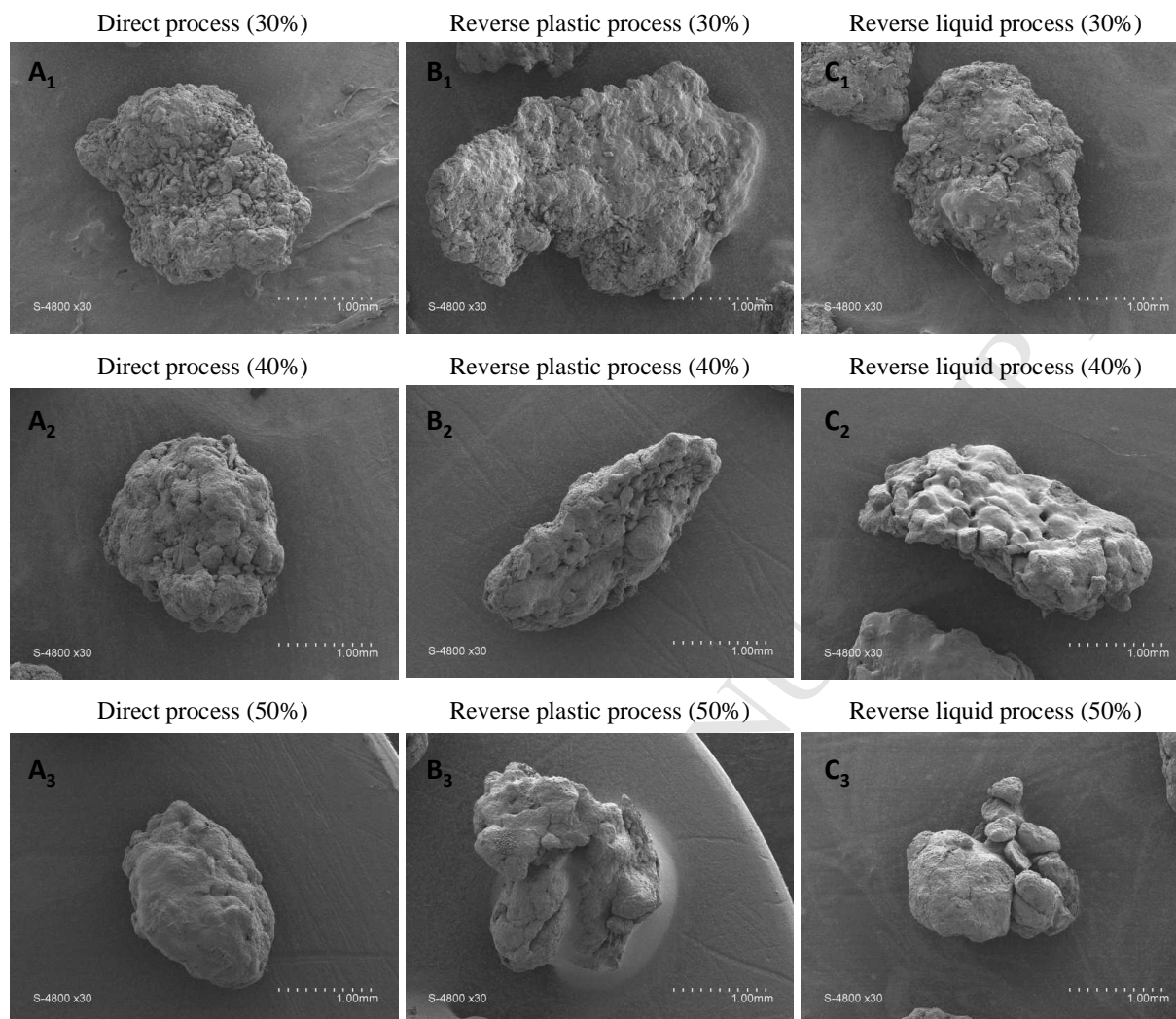


Figure 12: Microstructure by SEM of the dried agglomerates produced by the different process (direct, reverse plastic, or reverse liquid process) at the different process water content (at 30, 40, or 50%).

ACCEPTED

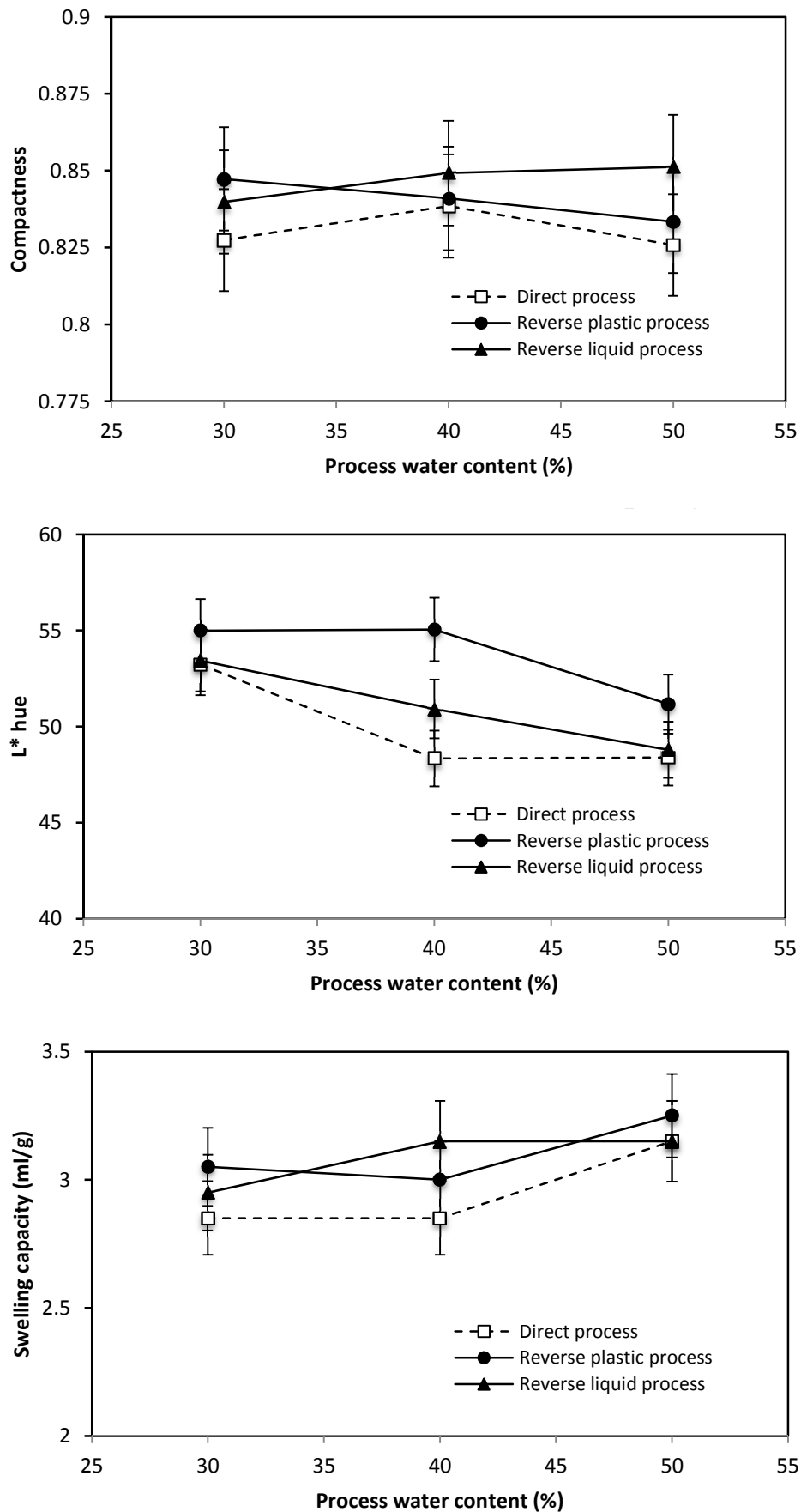


Figure 13: Impact of the process water content on the properties (compactness, color characteristics and the swelling properties) of the dried agglomerates, produced by the different processes.

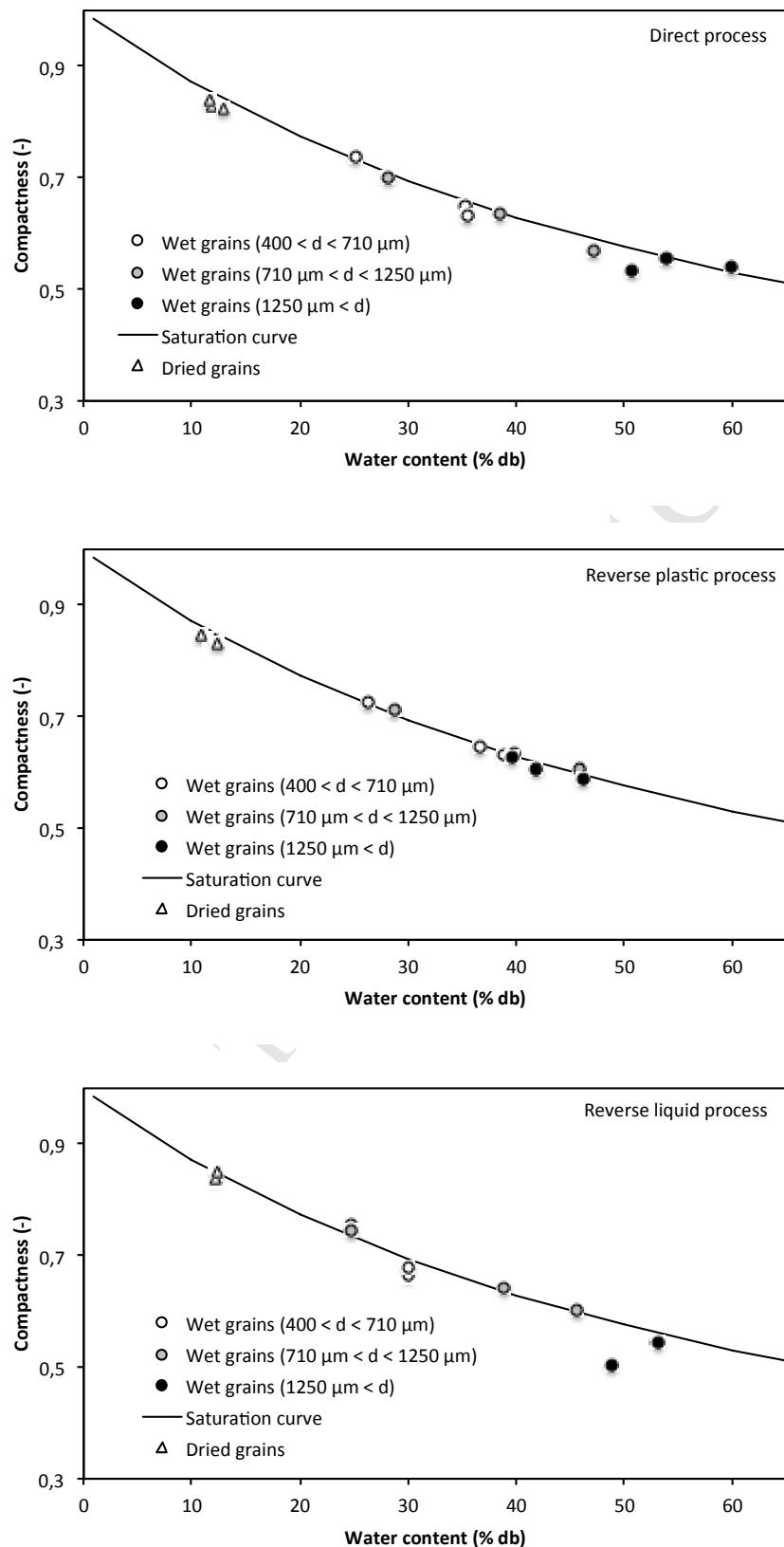


Figure 14: Hydro-textural description (compactness vs. measured water content) of the wet agglomerates and of the dried agglomerates, produced by the different processes (direct, reverse plastic, or reverse liquid processes).

Highlights

Innovative process to agglomerate wheat powder

Agglomerates were produced by the novel reverse wet agglomeration process.

The process conditions control the properties of the agglomerates.

The agglomeration process is mainly promoted by fragmentation mechanism.

ACCEPTED MANUSCRIPT